JOURNAL OF MATERIALS SCIENCE 20 (1985) 1725–1732

Static fatigue of thermoplastic elastomers

K. FUKUMORI, T. KURAUCHI
Toyota Central Research and Development Laboratories, Inc., Nagakute-cho, Aichi-gun, Aichi-ken 480-11, Japan

The failure behaviour in static fatigue of thermoplastic elastomers was estimated on the basis of the stochastic theory proposed for the failure of rubber vulcanizates. A statistical analysis of lifetime distributions for a styrene–butadiene–styrene triblock copolymer (SBS) in creep and stress relaxation experiments was made by using a Weibull distribution, and the failure behaviour of SBS was related to morphological changes of structure in stretched states, observed with a transmission electron microscope. Wear-out failure, in which the failure rate increases with time, occurs in the creep and stress-relaxation processes, and is similar to that in a carbon-reinforced rubber vulcanizate. These results suggest that in SBS, polystyrene (PS) domains dispersed in a continuous polybutadiene matrix serve as physical crosslinks and reinforcing fillers. In the stress relaxation process, however, the increased energy dissipation caused by plastic deformation and disruption of the PS domains leads the material to be more stabilized at a constant stretch ratio. This prolongs the lifetime of the material, due to multi-crack initiation at many portions of a specimen. The differences between the failure behaviour of SBS and that of the rubber vulcanizates are mainly caused by morphological changes of the structure in SBS on deformation.

1. Introduction

Thermoplastic elastomers, which have intermediate engineering properties between those of plastics and rubbers, have recently been widely used in engineering practice. The characteristic features of a thermoplastic elastomer are that it can exhibit rubber elasticity at ambient temperature without the process of vulcanization, it softens at elevated temperatures, and it can be processed in the same way as a conventional thermoplastic. An A–B–A type of block copolymer is one of the most typical thermoplastic elastomers, in which the central elastomeric B block is bonded on both ends to rigid A blocks, as shown schematically in Fig. 1. As seen in this figure, the A and B blocks are mutually incompatible and aggregate into two distinct phases. In this system, the A block acts as both a physical crosslink and a filler [1–5].

There have been many studies of the time-dependent structure–property relationships of thermoplastic elastomers, with particular emphasis on those of the A–B–A type of block copolymers [6–16]. As for the failure behaviour of thermoplastic elastomers, previous studies have focused mainly on the ultimate tensile properties of these materials [12–16]. Smith *et al.* [13–15] investigated the ultimate tensile properties of an elastomeric styrene–butadiene–styrene triblock copolymer (SBS) at various temperatures and various strain rates. They found that the time and temperature dependence of the mechanical properties of the material resulted mainly from the viscoelastic characteristics of the polystyrene (PS) domains, and that the plastic characteristics of the PS domains have some effect on the ultimate tensile properties of the material. Beecher *et al.* [12] examined the morphological changes of the structure in SBS on deformation, observed with the transmission electron microscope (TEM), which were related to the high strength of the material. They suggested that the high strength of the material originates from the inelastic deformation of the PS domains, in which large amounts of strain energy are dissipated, associated with the more even redistribution of the remaining strain in the material.

0022–2461/85 $03.00 + .12

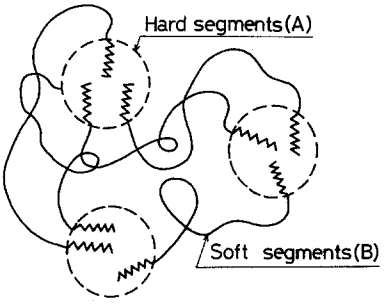

Figure 1 Schematic representation of phase arrangement in an *A–B–A* type of block copolymer.

However, there have been few reports on the failure behaviour of SBS in creep and stress relaxation processes, i.e. static fatigue. In this work, the static fatigue of SBS was studied and analysed by a statistical method which has already been applied to the failure behaviour of rubber vulcanizates [17, 18]. In addition, the morphologies of SBS in both unstretched and stretched states were observed with the TEM, and were related to the failure behaviour of the material. The failure behaviour in static fatigue of SBS was then estimated, and compared with that of rubber vulcanizates.

2. Experimental details

2.1. Material

The SBS used in this study was Cariflex TR4113 (Shell Chemical Co.; weight-average molecular weight of 8.0×10^4, 38 wt% styrene). Thirty sheets (150 x 150 mm) of about 1 mm thickness were prepared by compression moulding at 120° C for 5 min. Typical ring specimens (18.6 mm inside diameter, 20.0 mm outside diameter) were first punched out from each sheet, and the stress–strain curves of them were examined and checked. If the stress values at a stretch ratio, λ, of 8.0 were not within ± 2% of the mean value (the mean breaking stretch ratio was about 11.5) the sheet in question was not used in static fatigue experiments. Further ring specimens were punched out from the sheets which passed this initial test.

2.2. Static fatigue experiments

Static fatigue experiments involving creep and stress relaxation were carried out at 23° C under ambient atmosphere, and the lifetime up to the breaking point, t_B, was measured. The apparatus used for the measurement of the lifetime is the same with that is shown in our previous paper [18].

TABLE I Test conditions for SBS (TR4113)

Creep: engineering stress, σ_e (MPa)	1.96, 3.92 2.94 –
Stress relaxation: stretch ratio, λ	7.0, 9.0, 8.0, 10.0

In the creep experiment, all the ring specimens were weighed and the cross-sectional area of them were calculated from their weights, where the density of the material and the inside and outside diameters of the ring specimen were known. A constant engineering stress (based on undeformed cross-sectional area), σ_e, was then applied to a specimen with the use of a dead load, in which the load for each specimen was adjusted to provide a constant engineering stress by the use of correction weights. In the stress relaxation experiment, a specimen was held at a constant stretch ratio, λ. The test conditions are shown in Table I. The measurement of the lifetime was performed on twenty specimens, which were randomly sampled from all the ring specimens, under each test condition. The creep and stress relaxation properties of SBS were also measured.

2.3. Observation of fracture surfaces and deformation morphology

Fracture surfaces of specimens, which were coated with gold, were observed with a scanning electron microscope (SEM). The morphology of SBS both in the unstretched state and in stretched states of various stretch ratios was observed with a TEM. For these observations, ring specimens stretched to a constant stretch ratio, λ, were fixed to a metal frame, and then stained with osmium tetroxide vapour for 48 h at room temperature. The stained specimens were cut into a ribbon shape, and were embedded in epoxy resin. Ultrathin sections were made by cutting the embedded specimens parallel to the stretching direction.

3. Results and discussion

3.1. Statistical analyses of failure behaviours

A statistical analysis of lifetime distributions for SBS in the creep and stress relaxation experiments was made by using a Weibull distribution [19], on the basis of the stochastic theory for the failure behaviour of rubber vulcanizates proposed by Kawabata [17] and Fukumori and Kurauchi [18].

In this theory the probability of survival, $R(t)$,

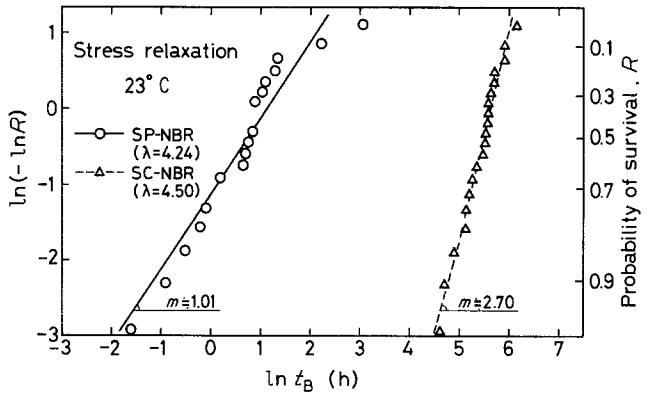

Figure 2 Typical Weibull plots of the distribution of the lifetime, t_B, in stress relaxation for pure acrylonitrile–butadiene rubber (NBR) vulcanizate (SP–NBR) and carbon-reinforced NBR vulcanizate (SC–NBR) [18]. λ = stretch ratio. Values of the Weibull modulus, m, were evaluated by least-squares analysis.

is given by

$$R(t) = \exp\left[-\left(\frac{t}{\beta}\right)^m\right] \quad (1)$$

where t is time, and β and m are constants. Hence, from Equation 1, the transition probability, or the failure rate, $\mu(t)$, is obtained as

$$\mu(t) = \frac{-\mathrm{d}R(t)/\mathrm{d}t}{R(t)} = \frac{mt^{m-1}}{\beta^m} \quad (2)$$

The failure rate, $\mu(t)$, indicates three types of failure mode corresponding to the values of m in Equation 2 as follows [20]:

$m = 1$	random failure; $\mu(t)$ is constant against time
$m > 1$	wear-out failure; $\mu(t)$ increases with time
$m < 1$	initial failure; $\mu(t)$ decreases with time

Thus, by the equation of m (the Weibull modulus) the failure mode can be determined. Equation 1 is transformed into

$$\ln[-\ln R(t)] = m\ln t - m\ln\beta \quad (3)$$

From the slope of $\ln[-\ln R(t)]$ plotted against $\ln t$, i.e. the Weibull plot, the value of m can be determined.

Fig. 2 shows typical Weibull plots of the distribution of the lifetime, t_B, for stress relaxation experiments on a pure rubber vulcanizate and a carbon-reinforced rubber vulcaizate [18]. As seen in this figure, observed values for each material appear to fit a straight line well. The value of m is nearly equal to 1.0 for the pure rubber vulcanizate, while the value of m for the carbon-reinforced rubber vulcanizate is larger than 1.0. Thus we concluded that in the pure rubber vulcanizate, random failure ($m = 1$) occurs, followed without delay by the initiation and propagation of an unstable crack; and that in the carbon-reinforced rubber vulcanizate, wear-out failure ($m = 2.70$) occurs, due to energy dissipation or the spatial effect near the tips of growing cracks in the presence of carbon black particles. In this case, multi-crack initiation plays an important role to delay the initiation of the critical crack and the propagation of growing cracks [18]. Hence, to compare the failure behaviour of SBS with that of the rubber vulcanizates, the Weibull plots of the lifetime distributions for SBS under all test conditions were examined in a similar manner to that shown in Fig. 2.

Figs. 3 and 4 show the Weibull plots of the distributions of the lifetime, t_B, for SBS in the

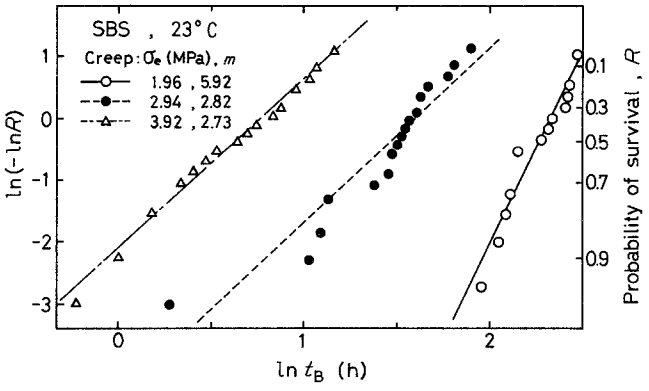

Figure 3 Weibull plots of the distribution of the lifetime, t_B, in creeep for SBS. σ_e = engineering stress, m = Weibull modulus.

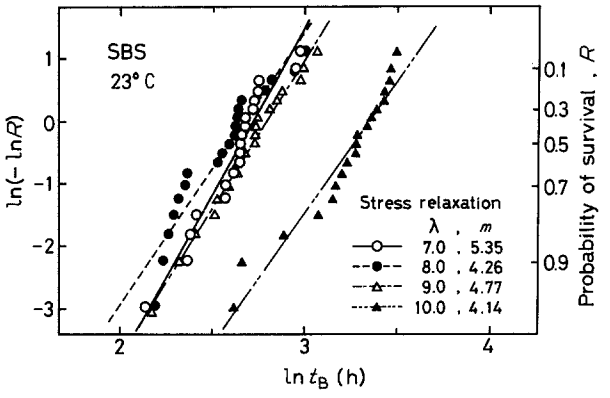

Figure 4 Weibull plots of the distribution of the lifetime, t_B, in stress relaxation for SBS. λ = stretch ratio, m = Weibull modulus.

creep and the stress relaxation experiments respectively. As seen in Fig. 3, the values of m in the creep experiment are larger than unity at various engineering stresses, σ_e. Hence, it is proved that the failure behaviour of SBS in the creep process is of the wear-out type ($m > 1$), similar to that of the carbon-reinforced rubber vulcanizate; this implies that the PS domains in the continuous polybutadiene (PB) matrix may serve as both physical crosslinks and reinforcing fillers. On the other hand, as seen in Fig. 4, the values of m in the stress relaxation experiment are also larger than unity at all values of stretch ratio, λ. However, it is known that there are many differences between the failure behaviour in the creep process and that in the stress relaxation one: the lifetime distributions in the stress relaxation experiment at stretch ratios of 7.0, 8.0 and 9.0 are almost the same, but the lifetime at a stretch ratio of 10.0 is longer than that at any lower stretch ratio. It has never been observed for rubber vulcanizates that the lifetime becomes longer at some higher stretch ratio.

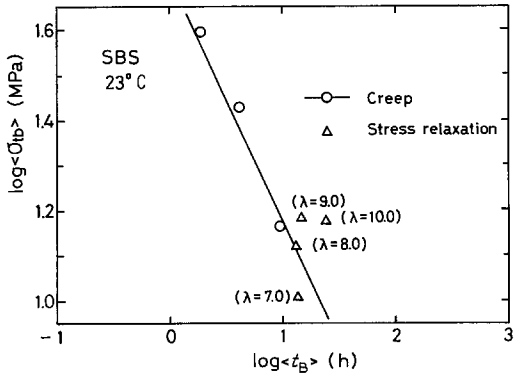

Figure 5 Plots of log $\langle\sigma_{tb}\rangle$ against log $\langle t_B\rangle$ for SBS in creep and stress relaxation. $\langle\sigma_{tb}\rangle$ = mean true breaking stress, $\langle t_B\rangle$ = mean lifetime, λ = stretch ratio.

Fig. 5 shows the dependence of the mean lifetime, $\langle t_B\rangle$, on the mean true breaking stress, $\langle\sigma_{tb}\rangle$, in the creep and stress relaxation experiments. In this figure, on the basis of the theory proposed for rubber vulcanizates [17, 18], $\log\langle\sigma_{tb}\rangle$ is plotted against $\log\langle t_B\rangle$ for SBS. As seen in the figure, the plot for SBS in the creep experiment follows a straight line in accordance with the results for rubber vulcanizates. On the other hand, the plot for SBS in the stress relaxation experiment deviates greatly from a linear relationship. Moreover, in the stress relaxation experiment the mean true breaking stress, $\langle\sigma_{tb}\rangle$, at a stretch ratio of 10.0 is a little lower than that at 9.0.

Thus, from the results for SBS mentioned above, we consider that the true stress in the stress relaxation process may decrease rapidly at large deformation, associated with a change of structure in SBS which causes energy dissipation in the material and leads it to be more stabilized. This energy dissipation mechanism due to the change of structure probably makes the differences between the failure behaviour of SBS and that of the rubber vulcanizates.

3.2. Creep and stress relaxation properties

The creep property, $\lambda(t)$, and the stress relaxation property, $\sigma_e(t)$, are empirically approximated by the following equations [17]:

$$\lambda(t) = \lambda_0 t^{k_c} \quad (4)$$

for the case of large λ, and

$$\sigma_e(t) = \sigma_0 t^{k_r} \quad (5)$$

where λ_0, σ_0, k_c and k_r are constants. The values of k_c (the creep rate) and k_r (the stress relaxation rate) were obtained from the expeimental data under all the test conditions, and are plotted against $\log\langle t_B\rangle$ in Fig. 6. As seen in this figure,

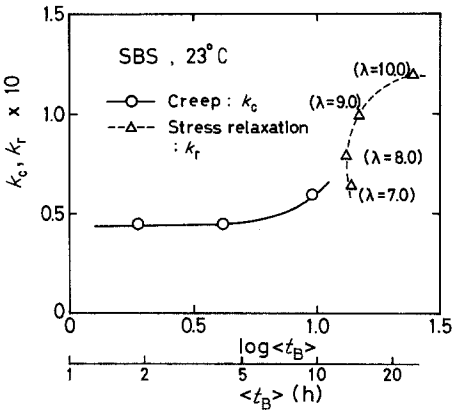

Figure 6 k_c and k_r plotted against $\langle t_B \rangle$ for SBS, k_c = creep rate, k_r = stress relaxation rate, $\langle t_B \rangle$ = mean lifetime.

the value of k_c increases with increasing $\langle t_B \rangle$ in the creep process, and the value of k_r increases remarkably with increasing $\langle t_B \rangle$ in the stress relaxation process. These results for SBS, especially in the stress relaxation process, are quite contrary to those for carbon-reinforced rubber vulcanizate, in which the mean lifetime decreases with increasing k_c or k_r [18]. The results for the carbon-reinforced rubber vulcanizate have been reasonably explained as follows: an irreversible change of the structure occurs rapidly after the first application of high strain, and is associated with the initiation of submicro-cracks caused by the progressive detachment of weak bondings with carbon black particles. The irreversible change of structure was in this case related to the increment in k_r.

Thus, we consider that there are some differences between the stress relaxation mechanism in SBS and that in the carbon-reinforced rubber vulcanizate, and that a high energy dissipation (due to the different relaxation mechanism) contributes to the release of stress concentration in SBS, and prolongs the lifetime of the material.

3.3. Fracture surfaces

Typical fracture surfaces of SBS in the creep and stress relaxation experiments, observed with an SEM, are shown in Fig. 7. As seen in Figs. 7a and b, the features of the fracture surfaces of SBS in both processes may be too complicated to discuss in detail from the standpoint of fractography.

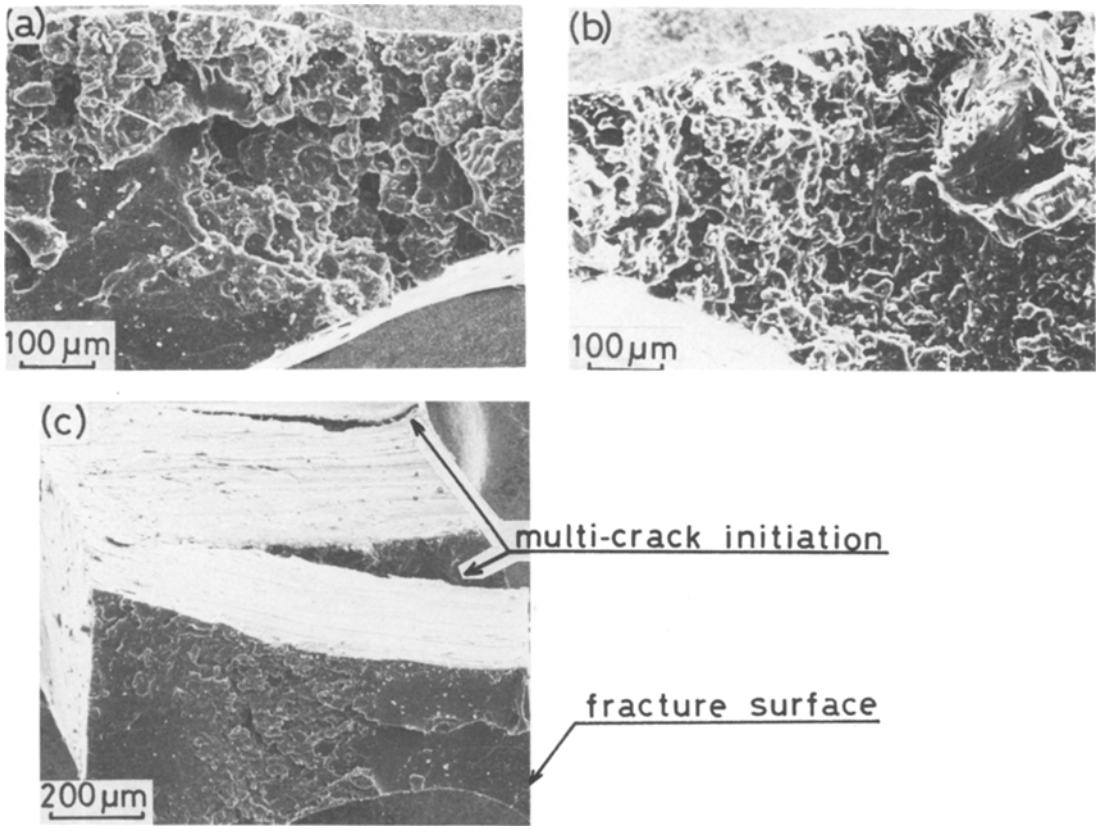

Figure 7 SEM images of fracture surfaces of SBS in (a) creep; (b), (c) stress relaxation.

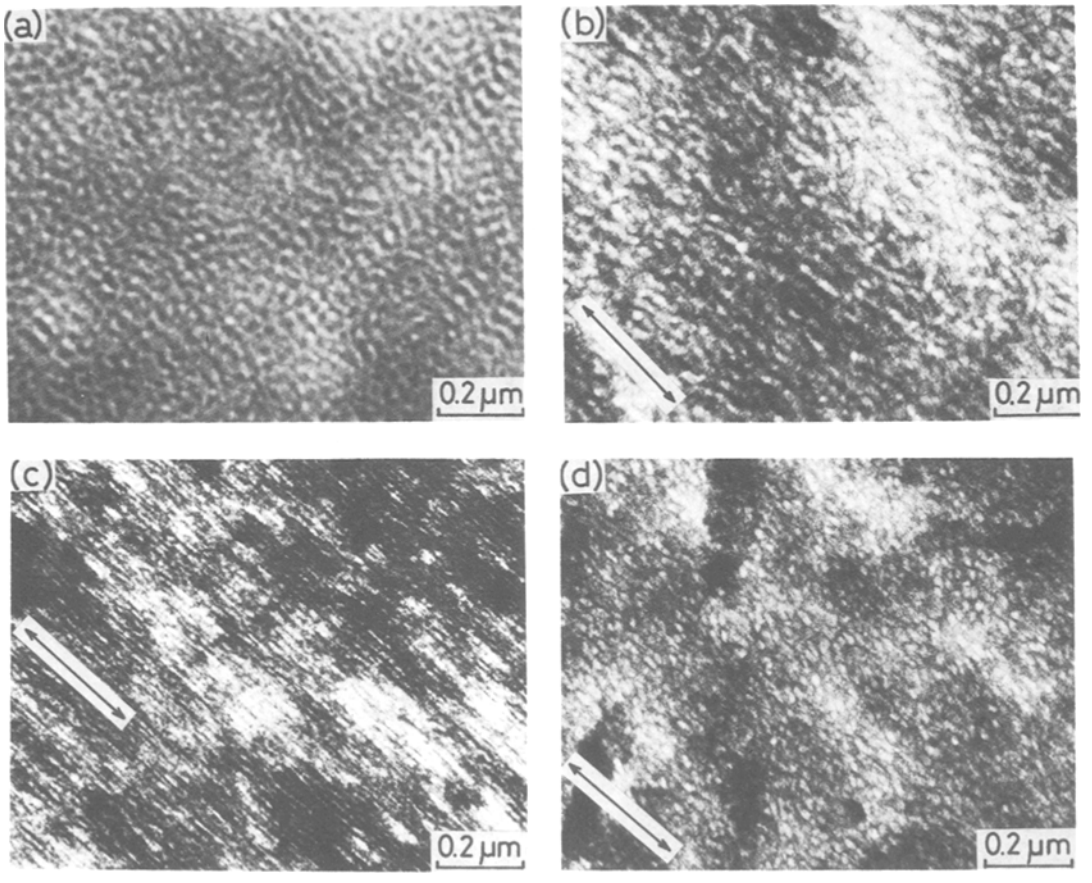

Figure 8 TEM images of ultrathin sections of SBS specimens: (a) unstretched; (b) stretched to $\lambda = 7.0$; (c) stretched to $\lambda = 9.0$; (d) stretched to $\lambda = 10.0$. Arrows indicate the stretching direction.

Moreover, as seen in Fig. 7c, multi-cracks initiate at many portions of a specimen in the stress relaxation process. We suggest that the multi-crack initiation mechanism also contributes to energy dissipation in the material, especially at large deformation in the stress relaxation experiment.

3.4. Change of morphology on deformation

Fig. 8 shows TEM images of ultrathin sections of ring specimens of SBS in both the unstretched and stretched states. As shown in Fig. 8a, the Cariflex TR4113 specimen as moulded by compression moulding in the unstretched state has a heterogeneous structure, in which the PS spheres are randomly dispersed in the continuous PB matrix and are interconnected to form a short rod-like structure or in some degree a reticular one. The morphologies of SBS in the stretched state at stretch ratios of 7.0, 9.0 and 10.0 are shown in Figs. 8b–d respectively. As seen in Fig. 8b, at a stretch ratio of 7.0 the short rod-like strings of PS spheres become aligned in the stretching direction with the orientation of the PB chains. At a stretch ratio of 9.0 (Fig. 8c) the PS domains are oriented in the stretching direction and become more ellipsoidal, so that the PB chains may become fully oriented. At a stretch ratio of 10.0 (Fig. 8d) the interconnected PS spheres eventually break up into individual particles, i.e. spherical domains, while the PB chains remain oriented in the stretching direction. We consider that considerable dissipation of the mechanical energy stored through stretching occurs due to the disruption of interconnections between the PS spheres; and that during the application of mechanical energy through stretching, the lower energy-requirement for the disruption of weak interconnections may be met sooner than the high energy-requirement for the scission of PB chains.

Thus, we estimate that increased energy dissipation, caused by the disruption of PS domains, may relieve local stress concentrations, delay the

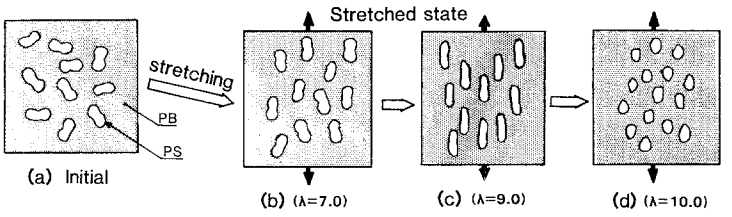

Figure 9 Schematic representation of morphological changes in the structure of SBS on deformation: (a) short rod-like PS domains randomly dispersed in PB matrix; (b) alignment of PS domains in the stretching direction; (c) orientation and deformation of PS domains in the stretching direction; (d) disruption of short rod-like PS domains into spherical domains. PS = polystyrene, PB = polybutadiene.

initiation of a critical crack or the propagation of growing cracks, and prolong the lifetime of the material. On the other hand, the PB chains are still oriented, and this may be followed by the formation of localized heterogeneous regions of lower density in the PB matrix. We believe that in the lower-density regions, microvoids occur and ultimately grow to form a crack. The formation of the lower-density regions in elastomeric block copolymers was proposed by Inoue *et al.* [16], who investigated the deformation mechanism of elastomeric block copolymers by means of simultaneous measurements of tensile stress–strain relations, small-angle light scattering and small-angle X-ray scattering.

In the stress relaxation process, the true stress decreases monotonously with time at a constant stretch ratio. Hence, the energy dissipation associated with the change of morphology at large deformation leads the material to be more stabilized, as long as the strain is held constant. Dangling fragmented PS domains or lower-density regions in the PB matrix may be regarded as relatively stable for the initiation of a critical crack in the stress relaxation process, and the initiation of multi-cracks occurs more frequently in comparison with that in the creep process mentioned above.

On the other hand, in the creep process the true stress increases monotonously with time, which is similar to the dependence of stress on strain under tension. Hence, the change in morphology at large deformation, caused by the plastic flow and disruption of the PS domains, progresses steadily with time. Eventually, microvoids may possibly occur in lower-density regions of the matrix, and grow to some critical size, accompanied by the initiation of cracks over fewer portions of the specimen compared with that in the stress relaxation one.

Thus we concluded that the differences between the failure behaviour of SBS and that of rubber vulcanizates may be caused by characteristic changes in the morphology of SBS on deformation, especially in the stress relaxation process, and that the controlling step in the overall failure process of SBS may involve plastic deformaion and disruption of the PS domains, associated with much energy dissipation.

4. Conclusions

The failure behaviour in static fatigue of thermoplastic elastomers has been studied by statistical analysis of lifetime distributions, on the basis of the stochastic theory proposed for rubber vulcanizates; this was related to the change of morphology in the stretched state observed with a TEM. The differences between the failure behaviour of thermoplastic elastomers and that of rubber vulcanizates were then discussed.

In the thermoplastic elastomers, wear-out failure ($m > 1$) occurs in both creep and stress relaxation processes; it is associated with multi-crack initiation in which a plastic component dispersed in a matrix of rubbery component serves as both physical crosslinks and reinforcing fillers, in a similar manner to that in carbon-reinforced rubber vulcanizate. In the stress relaxation process, however, increased energy dissipation is caused by plastic deformation and disruption of the domain structures at large deformation; this prolongs the lifetime of the material at constant stretch ratio, in contrast with the results for rubber vulcanizates. The morphological changes in these materials on deformation, accompanied by the alignment and orientation of plastic domains in the stretching direction and the disruption of the domains, are illustrated scheematically in Fig. 9. In thermoplastic elastomers, the rubbery chains become possibly more highly oriented on deformation than those in the rubber

vulcanizates, so that this contributes to the high strength of the former.

We concluded from these results that the differences between the failure behaviour of thermoplastic elastomers and that of rubber vulcanizates are mainly caused by the morphological changes of thermoplastic elastomers on deformation.

Acknowledgements

The authors are indebted to Dr O. Kamigaito for valuable discussions. They also thank Mr N. Suzuki for taking the TEM images of SBS.

References

1. G. HOLDEN, E. T. BISHOP and N. R. LEGGE, *J. Polym. Sci. Part C* **26** (1969) 37.
2. J. A. MANSON and L. H. SPERLING, "Polymer Blends and Composites" (Plenum Press, New York, 1976) p. 121.
3. M. MORTON, *J. Polym. Sci.* Symposium No. 60 (1977) 1.
4. J. C. WEST and S. L. COOPER, in "Science and Technology of Rubber" edited by F. R. Eirich, (Academic Press, New York, 1978) p. 531.
5. M. SHEN and H. KAWAI, *Amer. Inst. Chem. Engrs. J.* **24** (1978) 1.
6. D. M. BRUNWIN, E. FISCHER and J. F. HENDERSON, *J. Polymer Sci. Part C* **26** (1969) 135.
7. D. G. FESKO and N. W. TSCHOEGL, *ibid.* **35** (1971) 51.
8. D. H. KAELBLE, *Trans. Soc. Rheol.* **15** (1971) 235.
9. D. H. KAELBLE and E. H. CIRLIN, *J. Polym. Sci.* Symposium No. 43 (1973) 131.
10. M. SHEN and V. A. KANISKIN, *J. Polym. Sci. Polym. Phys. Ed.* **11** (1973) 2261.
11. J. A. ODELL and A. KELLER, *Polym. Eng. Sci.* **17** (1977) 544.
12. J. F. BEECHER, L. MARKER, R. D. BRADFORD and S. L. AGGARWAL, *J. Polym. Sci. Part C* **26** (1969) 117.
13. T. L. SMITH and R. A. DICKIE, *ibid.* **26** (1969) 163.
14. T. L. SMITH, in "Block Polymers", edited by S. L. Aggarwal (Plenum Press, New York, 1970) p. 137.
15. *Idem, J. Polym. Sci., Polym. Phys. Ed.* **12** (1974) 1825.
16. T. INOUE, M. MORITANI, T. HASHIMOTO and H. KAWAI, *Macromolecules* **4** (1971) 500.
17. S. KAWABATA, in "Durability of Macromolecular Materials", edited by R. K. Eby, ACS Symposium Series 95 (American Chemical Society, Washington, D. C., 1979) p. 261.
18. K. FUKUMORI and T. KURAUCHI, *J. Mater. Sci.* **19** (1984) 2501.
19. W. WEIBULL, "Fatigue Testing and Analysis of Results" (Pergamon Press, New York, 1961) p. 143.
20. J. H. K. KAO, *J. Amer. Statis. Assoc.* **51** (1956) 514.

Received 2 April
and accepted 26 July 1984